Inhibition of the Myotoxicity Induced by *Bothrops jararacussu* Venom and Isolated Phospholipases A₂ by Specific Camelid Single-Domain Antibody Fragments

Nidiane D. R. Prado[1], **Soraya S. Pereira**[1], **Michele P. da Silva**[1], **Michelle S. S. Morais**[1], **Anderson M. Kayano**[1], **Leandro S. Moreira-Dill**[1], **Marcos B. Luiz**[1], **Fernando B. Zanchi**[1], **André L. Fuly**[2], **Maribel E. F. Huacca**[3], **Cleberson F. Fernandes**[4], **Leonardo A. Calderon**[1,3], **Juliana P. Zuliani**[1,3], **Luiz H. Pereira da Silva**[1†], **Andreimar M. Soares**[1], **Rodrigo G. Stabeli**[1,3], **Carla F. C. Fernandes**[1,5]*

1 Fundação Oswaldo Cruz, Fiocruz Rondônia, Porto Velho-RO, Brazil, **2** Universidade Federal Fluminense, UFF, Rio de Janeiro-RJ, Brazil, **3** Universidade Federal de Rondônia, UNIR, Porto Velho-RO, Brazil, **4** Empresa Brasileira de Pesquisa Agropecuária, Embrapa, Porto Velho-RO, Brazil, **5** Centro de Pesquisa em Medicina Tropical, CEPEM, Porto Velho-RO, Brazil

† Deceased.
* carlaceledonio@fiocruz.br

Abstract

Antivenoms, produced using animal hyperimmune plasma, remains the standard therapy for snakebites. Although effective against systemic damages, conventional antivenoms have limited efficacy against local tissue damage. Additionally, the hypersensitivity reactions, often elicited by antivenoms, the high costs for animal maintenance, the difficulty of producing homogeneous lots, and the instability of biological products instigate the search for innovative products for antivenom therapy. In this study, camelid antibody fragments (VHH) with specificity to Bothropstoxin I and II (BthTX-I and BthTX-II), two myotoxic phospholipases from *Bothrops jararacussu* venom, were selected from an immune VHH phage display library. After biopanning, 28 and 6 clones recognized BthTX-I and BthTX-II by ELISA, respectively. Complementarity determining regions (CDRs) and immunoglobulin frameworks (FRs) of 13 VHH-deduced amino acid sequences were identified, as well as the camelid hallmark amino acid substitutions in FR2. Three VHH clones (KF498607, KF498608, and KC329718) were capable of recognizing BthTX-I by Western blot and showed affinity constants in the nanomolar range against both toxins. VHHs inhibited the BthTX-II phospholipase A₂ activity, and when tested for cross-reactivity, presented specificity to the *Bothrops* genus in ELISA. Furthermore, two clones (KC329718 and KF498607) neutralized the myotoxic effects induced by *B. jararacussu* venom, BthTX-I, BthTX-II, and by a myotoxin from *Bothrops brazili* venom (MTX-I) in mice. Molecular docking revealed that VHH CDRs are expected to bind the C-terminal of both toxins, essential for myotoxic activity, and to epitopes in the BthTX-II enzymatic cleft. Identified VHHs could be a biotechnological tool to improve the treatment for snake envenomation, an important and neglected world public health problem.

Introduction

Snakebites represent a relevant public health problem, especially in subtropical and tropical countries. Affecting mainly the rural population, about 5 million snakebites occur each year worldwide, causing approximately 100,000 deaths [1–3]. A large number of the victims experience permanent physical sequelaes due to inflammatory, hemorrhagic, coagulant, neurotoxic and myotoxic effects occasioned by the venom components. These signs are often aggravated by the difficulty of accessing health services in less developed regions [2,4].

It has been described that, worldwide, there are four families of venomous snakes, i.e. Viperidae, Elapidae, Atractaspididae, and Colubridae [5]. Viperidae and Elapidae families cause the most venomous bites. Beloging to the Viperidae family, the *Bothrops* genus is responsible for the majority of snake envenoming in Central and South America, occasioning both high morbidity and mortality [6].

Diagnosis of snakebite is based on clinic-epidemiological evelution and the current treatment consists, besides supportive care, of the intravenous administration of antivenoms [7]. To manufacture antivenom, hyperimmune plasma is obtained from venom-immunized horses or sheep and subjected to physical and chemical processes to generate monovalent or polyvalent serum, containing polyclonal immunoglobulins G (150 kDa) or antibody fragments, such as F (ab')$_2$ (100 kDa) or Fab (50 kDa), which are not affinity purified [8].

Although they are effective against systemic toxic effects, conventional antivenoms poorly neutralize venom toxins in deep tissues, due to the discrepancies between the pharmacokinetic profiles of the low molecular weight toxins and antivenoms [9]. Additionally, the hypersensitivity reactions, often elicited by heterologous serum, the high costs for animal maintenance, the difficulty of producing homogeneous lots, the instability of biological products, together with animal rights and welfare instigate the search for innovative products for snakebite therapy [8].

Among proposed innovations the use of monoclonal antibodies and recombinant antibody fragments, like single chain variable fragment (scFv), stand out [10–12]. While the high immunogenicity, as well as the high cost for monoclonal antibodies production limit the use of that technology, scFvs usually show lower affinity when compared with the antigen recognition region of conventional antibodies [13].

To overcome these issues, studies have proposed the use of recombinant antigen binding domains derived from camelid heavy chain antibodies, called VHH, for antivenom production [14]. With about 15 kDa, one-tenth the size of whole antibodies, VHH possess attractive physico-chemistry, pharmacokinetic and pharmacodynamic properties, and shows low immunogenicity. Besides conserving the conventional antibodies' benefits in terms of affinity and selectivity, they present high stability, solubility and lower production cost, when compared with human or murine antibodies [15]. VHHs present higher tissue penetration ability, and can act as potent enzyme inhibitors by penetrating in the toxin enzymatic clefts, normally inaccessible to conventional VHs [16,17]. Thus, VHHs have emerged as versatile biotechnological tools for antivenom development. However, antivenoms composed entirely of small antibody fragments, including VHHs, would have limited therapeutic efficacy because of their short serum half-life profiles. Therefore, different strategies have been explored in order to extend the serum half-life of VHHs [18]. Furthermore, the development of antivenoms based on a mixture of high (IgG; F(ab')2) and low (Fab, scFv, VHH) molecular mass antibodies, could help match the pharmacokinetic profiles of venoms, improving antivenom biodistribution, stability, and toxin neutralization while reducing side effects in humans. Besides allowing for the neutralization of toxins by small fragments in tissue compartments, the formed toxin-VHH complex can be eliminated rapidly through renal excretion. In addition, these preparations

ensure that a significant concentration of high molecular mass antibodies remains in circulation to neutralize toxins later in the course of envenomation [14].

For VHH production, two myotoxic phospholipases A_2 (PLA$_2$), obtained from *B. jararacussu* venom, were used as antigens. BthTX-I, a Lys-49 PLA$_2$-like, without enzymatic activity, and BthTX-II, an enzymatically active Asp-49 PLA$_2$. With 76% amino acid sequence similarity and a molecular mass of 14 kDa, both toxins correspond to 40–50% of the venom dry weight, and play an important role in muscle necrosis [19,20].

Evaluating the features of VHH, the characteristics of bothropstoxins, and the necessity for developing new approaches to support the treatment or even to diagnose snakebites, this study aimed to select VHHs capable of recognizing and neutralizing myotoxic effects triggered by BthTX-I, BthTX-II, and *B. jararacussu* venom.

Materials and Methods

Ethics statements

Experimental procedures involving animals were carried out in accordance with the recommendations of the National Council for the Control of Animal Experimentation (CONCEA), and were approved by the Ethics Commission on Animal Use (CEUA) of Fiocruz Rondônia under protocol 2012/11. Animal health status was checked routinely by a veterinary. In order to verify the study viability and to determine a protocol for experimental humane endpoints, a pilot study was conducted previously, following the CONCEA Normative Resolution No. 23, of July 23, 2015 (http://www.mct.gov.br/upd_blob/0237/237231.pdf). This protocol was conducted when severe neurotoxic and myotoxic signs were observed. All mice groups were monitored regularly (5 min intervals) until the end of experimental period and there were no unintended death of animals. After topical anesthesia (tetracaine ophthalmic drops) for retro-orbital bleeding, all animals were euthanized by Cervical dislocation, according to CONCEA Normative Resolution No. 13, of September 20, 2013 (http://www.mct.gov.br/upd_blob/0228/228451.pdf). The licenses related to access to Brasilian genetic resources for scientific purposes are: Instituto Brasileiro do Meio Ambiente e dos Recursos Naturais Renováveis–IBAMA, Instituto Chico Mendes de Conservação da Biodiversidade–ICMBio (Number: 27131–1) and Conselho de Gestão do Patrimônio Genético–CGEN/Brazil (Number 010627/2011-1).

Lama glama immunization and immune response monitoring

One young adult male *L. glama*, with food and water *ad libitum*, was immunized at fortnightly intervals seven times with 100 μg of each BthTX-I and BthTX-II [19] via subcutaneous injections. Animal immune response was monitored by enzyme immunoassay. The assay was performed in triplicate. For this, microtiter plates (Nunc-MaxiSorp) were coated with 1 μg BthTX-I or BthTX-II in PBS/well and incubated overnight at 4°C. Wells were washed with PBS/ 0.05% Tween-20 (PBST) and unspecific sites blocked with blocking solution (BS – 3% of BSA plus 1% of skimmed milk in PBS) for 3 h. Subsequently, serial dilutions (1:10^2; 1:10^3;1:10^4; 1:10^5) of the serum, collected each week, were added to the wells and the plates were incubated for 12 h in BS at 4°C. After washing with PBST, rabbit anti-llama IgG$_2$/IgG$_3$ [21] at a 1:12000 dilution in BS was added. Excess antibody was removed by washing, and peroxidase conjugated mouse anti-rabbit IgG (Sigma Aldrich) was incubated at a 1:40000 dilution for 2 h in BS. TMB-Ultra (Millipore) was used to reveal the reaction. Absorbances were measured at 450 nm in a microplate reader (BioTek-Synergy HT). The negative control was performed using the llama pre-immune serum.

VHH library construction

To construct the VHH immune library, blood was collected 3 days following the final boost, and lymphocytes were isolated with Ficoll-Paque Plus (GE Healthcare). Lymphocyte total RNA was extracted using Trizol Reagent (Invitrogen), and cDNA synthesis carried out with the SuperScript III First-Strand Synthesis System for RT-PCR (Invitrogen). Subsequently, PCR, performed using the cDNA as template and one pair of gene-specific primers, resulted in an amplification of the conventional and heavy-chain IgG repertoire gene fragments. Amplified gene fragments were electrophoresed and the purified heavy chain amplicon was used as template in a nested PCR, resulting in fragments consisting of about 400 bp [21]. VHH fragments were inserted into the **pHEN1-6xHis** phagemid vector, in frame with the M13 gene III for expression of VHH-6xHis-PIII fusion protein. Ligation products were transformed into electrocompetent *E. coli* TG1 (Stratagene) to generate the primary library of VHH. Library size was determined by plating the transformation product on 2YT agar plates with 100 μg/mL ampiclilin and 2% glucose (2YT/amp/glu). The attainment of recombinant M13KO7 phages (**New England Biolabs)** expressing anti-BthTX-I and anti-BthTX-II VHHs, as well as polyethylene glycol precipitation were performed as described by [22], and used for biopanning.

Screening for anti-BthTX-I and anti-BthTX-II VHHs

BthTX-I and BthTX-II were used separately to select specific VHH-phages. One milligram of each toxin was immobilized on MaxiSorb immunotubes (Sigma-Aldrich) overnight at 4°C. Excess BthTX-I and BthTX-II were washed with PBST and the reactions were blocked in BS for 2 h. Phages expressing VHH repertory, previously incubated in BS, were added to the immunotubes and the samples were incubated at 37°C. After washing, phage elution was performed with 100 mM HCl and the reaction was neutralized with 1 M Tris-HCl. The eluants were transferred, separately, to *E. coli* TG1 (A_{600} 0.5), and the cultures were incubated at 37°C. After centrifugation, the supernatants were discarded, the pellet resuspended in 2YT, plated on 2YT/amp/glu, and incubated overnight at 30°C. VHH presence in the selected clones was checked by colony PCR and positive clones were selected to verify antigen binding specificity by ELISA. Thus, clones were expressed in 2YT/amp plus 1 mM IPTG for 16 h at 30°C. Following centrifugation, 50 μL of supernatants containing soluble VHHs were used to perform ELISA assay, as described under immune response monitoring. Llama BthTX-I and BthTX-II immune serum was used as positive controls. The negative control was carried out using the llama pre-immune serum. Positive clones were sequenced, analyzed and submitted to GenBank.

Expression and Purification of anti-BthTX-I and anti-BthTX-II VHHs

To perform the expression of soluble VHHs, selected VHH-pHEN1-6xHis were electroporated into the non-supressor strain *E. coli* HB2151. Clones were grown in 2YT/amp (1 L) under shaking at 37°C (A_{600} = 0.5). To induce VHH expression, 1 mM IPTG was added to the reactions, and the cultures were grown for 16 h at 30°C. Samples were centrifuged, and individual pellets were resuspended in Tris-HCl (50 mM, pH 8.0), and treated with 1 mL of lysozyme (100 mg/mL). The sonication process was carried out for 3.5 min with 1 minute pulses at 20 kHz and an amplitude of 40 (Misonix Ultrasonic Processor, Qsonica). Samples were centrifuged, and purified by immobilized metal affinity chromatography (IMAC) using TALON® Superflow Resin (GE Healthcare). VHH protein concentration was determined by the Bradford method.

Western blot analysis

For the Western blot (WB) analysis, 10 µg of BthTX-I and BthTX-II were reduced, electrophoresed on a 15% SDS-PAGE, and transferred to a nitrocellulose membrane (Amersham Life Science). Reactive sites were blocked with 5% skimmed milk in TBS buffer (TBSM) at 4°C overnight. After washing with TBS/0.1% Tween 20 (TBST), the strips were incubated with 0.2 mg/mL of each anti-BthTX VHH (KF498607, KF498608, KC329715 and KC329718) overnight. Strips were washed with TBST and incubated with anti-His antibody (GE Healthcare) (1:3000 in 5% TBSM) for 16 h. After washing, the samples were incubated with HRP-conjugated anti-mouse IgG produced in goat (1:3000 in 5% TBSM). Strips were washed, and the reactive signals detected after incubation with hydrogen peroxide in diaminobenzidine (DAB) solution (SIGMA*FAST*™ DAB with Metal Enhancer Tablets, Sigma-Aldrich). Llama postimmunization serum (1:1000) was used as positive control. The negative control was performed with the llama pre-immune serum (1:1000).

Kinetic analysis

SPR spectroscopy was performed using a Biacore T200 system (GE Healthcare). BthTX-I and BthTX-II were immobilized on carboxymethylated dextran CM5 chips by amine coupling [23]. The dextran layer of the sensor chip was activated by a 1:1 (v/v) mixture of 0.4 M EDC (1-Ethyl-3-3-dimethylaminopropyl carbodiimide) and 0.1 M NHS (N-hidroxysuccinimide) at a flow rate of 5 µL/min. BthTX-I was diluted in sodium phosphate buffer (66 mM, pH 7) and injected into a selected the flow cell for surface immobilization, while BthTX-II was diluted in sodium acetate (10 mM, pH 5.5). After that, a solution of 1 M ethanolamine hydrochloride was injected in order to block remaining reactive groups in flow cell. The control flow cell was prepared only with ethanolamine. For kinetic measurements, CM5-BthTX-I and CM5-BthTX-II were subjected to serial dilutions of VHH (442.6 to 3.458 nM), and (1757.8 to 0.429 nM), respectively, into the running buffer (0.1 M phosphate buffer, 27 mM KCl and 1.37 M NaCl, pH 7.4). The kinetic assay was performed at a flow rate of 30 µL/min at 37°C. Chip regeneration was performed with AIW solution followed by ICW solution for 30 s each [**A**—Equal volumes of oxalic acid, H_3PO_4, formic acid, and malonic acid, each at 0.15 M, pH 5.0; **C**—20 mM EDTA; **I**—KSCN (0.46 M), $MgCl_2$ (1.83 M), urea (0.92 M), guanidine-HCl (1.83 M); **W**—deionized water] according to [24]. The binding responses were calculated by subtracting the RUs obtained from both blank control cell and running buffer injection. Kinetic analyses were performed by fitting the obtained sensograms with the 1:1 Langmuir model using the BIA-evaluation software (GE Healthcare).

Inhibition of phospholipase activity on fluorescent lipid

PLA_2 activity was measured using acyl-NBD PC substrate (Avanti Polar Lipids) through fluorescence intensity. The fluorescent phospholipid was reconstituted in chloroform and dried over a low flow of N_2. The dried phospholipid (Acyl-NBD-PC-1-acyl-2-{6-[(7-nitro-2-1,3-benzoxadiazol-4-yl)amino]hexanoyl}-sn-glycero-3-phosphocholine) was dissolved in 150 mM NaCl, and a stock phospholipid solution of 1 mg/mL was obtained and used throughout the experiments [25]. Assays were performed in a final volume of 150 µL in Fluorescence Spectrometer Spectra Max M4 (Molecular Devices, Sunnyvale, CA)—Software SoftMax 6.0 at 37°C in opaque plates at excitation and emission wavelengths of 460 nm and 534 nm, respectively, at an interval of 3 s between each read, over 5 min. The standard reaction medium contained 20 mM Tris–HCl pH 7.5, 8 mM $CaCl_2$ and 5 µM of phospholipid. To verify VHH's ability to inhibit BthTX-II phospholipase activity, 0.06 µg of the toxin was pre-incubated with selected VHHs (1:5; 1:10 and 1:40 w/w) for 30 min at 37°C. As a positive control the standard reaction

with only BthTX-II (0.06 µg) was used. The reaction produced 220 fluorescence units, corresponding to 100% of PLA$_2$ activity. The negative control was carried out in the absence of BthTX-II.

Cross reactivity of anti-BthTX VHHs

The cross reactivity of selected VHHs was analyzed by ELISA. For this, microplates were coated separately with 500 ng of snake venoms (Serpentário de Proteínas Bioativas, Batatais, Brazil) from twenty-two different species (*B. alternatus*, *B. atrox*, *B. bilineata*, *B. brazili*, *B. diporus*, *B. insularis*, *B. jararaca*, *B. leucurus*, *B. marajoensis*, *B. matogrossensis*, *B. moojeni*, *B. pauloensis*, *B. pirajai*, *B. urutu*, *Calloselasma rhodostoma*, *Crotalus atrox*, *Crotalus durissus cascavella*, *C. d. collilineatus*, *C. d. cumanensis*, *C. d. terrificus*, *Micrurus spixii*), as well as seven different isolated toxins (PLA$_2$ from *B. atrox*, and PLA$_2$-I, convulxin, crotamin crotapotin, crotoxin, and giroxin from *C. d. terrificus*. After adsorption of the venom/toxins, plates were incubated at 4°C overnight, and washed with PBST. Nonspecific sites were blocked with BS for 2 h, washed with PBST, and 1 µg of purified VHH (pre-incubated in BS) was added. Plates were incubated overnight, washed with PBST and the anti-His antibody (1:5.000) was added. Goat anti-mouse IgG-HRP (1:10.000) was used as secondary antibody. Reactions were revealed with TMB, and measured at 450 nm. *B. jararacussu* venom, BthTX-I, and BthTX-II, positive controls, were used. For the negative control, ELISA wells were not adsorbed with venoms or toxins. The assay was performed in triplicate.

Neutralization of myotoxicity by *in vitro* pre-incubation

To evaluate the VHH neutralization effect on myotoxicity induced by *B. jararacussu* venom, BthTX-I and BthTX-II, animals were divided into 13 groups of 5 male mice (28–30 g). *B. jararacussu* venom, BthTX-I and BthTX-II were separately pre-incubated with VHH at 37°C for 1 h, according to Table 1. Then, each group received an i.m. injection of 50 µL in the gastrocnemius muscle. Positive control animals were injected with BthTX-I, BthTX-II or venom. Negative control animals received 50 µL of PBS or VHHs. After 3 h, blood was collected from the

Table 1. Groups of mice subjected to *in vivo* neutralization assays.

Group	Description	Administered dose	Molar ratio	Administered volume
01	PBS	-	-	50 µl
02	VHH KF498607	50 µg	-	50 µl
03	VHH KC329718	50 µg	-	50 µl
04	BthTX-I	10 µg	-	50 µl
05	BthTX-I + VHH KF498607	10 µg + 50 µg	1:5	50 µl
06	BthTX-I + VHH KC329718	10 µg + 50 µg	1:5	50 µl
07	BthTX-II	15 µg	-	50 µl
08	BthTX-II + VHH KF498607	15 µg + 75 µg	1:5	50 µl
09	BthTX-II + VHH KC329718	15 µg + 75 µg	1:5	50 µl
10	*B. jararacussu* venom	10 µg	-	50 µl
11	*B. jararacussu* venom + VHH KF498607	10 µg + 50 µg	-	50 µl
12	*B. jararacussu* venom + VHH KC329718	10 µg + 50 µg	-	50 µl
13	*B. jararacussu* venom + VHH KC329718	10 µg + 100 µg	1:10	50 µl
14	MTX-I	10 µg	-	50 µl
15	MTX-I + VHH KF498607	10 µg + 50 µg	1:5	50 µl
16	MTX-I + VHH KC329718	10 µg + 50 µg	1:5	50 µl

doi:10.1371/journal.pone.0151363.t001

orbital plexus to determine the creatine kinase activity using diagnostic kits (BIOCLIN, Belo Horizonte, MG). Results were expressed as CK U/L. To analyze the cross neutralization, 3 other groups of mice were treated with a myotoxic PLA$_2$ of *B. brazili* (MTX-I), in the presence or absence of VHHs.

Molecular docking and modeling

Homology modeling was carried out with 4 selected VHH clones. Protein Blast [26] and Protein Data Bank (PDB) were used for search and retrieval of the template structures. Sequence alignment was performed by ClustalW [27] and MODELLER v9.10 [28], which was also used for model building. A total of 1000 models were generated and the final model was selected based on the lowest DOPE scores calculated. The overall stereochemical quality of the final model for VHHs was assessed using the program PROCHECK [29]. Interactive visualization and comparative analysis of molecular structures were carried out on a Swiss-PDB viewer [30] and UCSF Chimera [31], and structure images were generated by Persistence of Vision Raytracer (POV-ray) 3.62 (http://www.povray.org). The ClusPro2.0 server (http://ClusPro.bu.edu/) [32] was used to predict the possible interactions between all VHH structures and BthTX-I (PDB accession code: 3HZD:A) [33] and BthTX-II (PDB accession code: 3JR8:A) [34]. The antibody mode was used with the non-CDR regions masked automatically [35]. VHHs were submitted as the receptor and the toxins as the ligand. The software identified the 1000 best scoring solutions and then clustered them according to RMSD considerations. Subsequently, the lowest ClusPro score, which represents the greatest probability of antigen-antibody interaction, was selected [36].

Results

L. glama immune response and selection of anti-BthTX VHHs

The llama humoral response was satisfactory, verified by an increase in the ability of postimmunization sera to bind to the antigens in the immunoenzymatic assays (data not shown). The final antiserum titre (Day 87) was determined as 1×10^5 for BthTX-I and BthTX-II. The Phage Display method was employed to select specific VHHs for both toxins. Prior to construction of an immune VHH library with 4×10^{12} clones, about 5×10^6 lymphocytes from immunized *L. glama* were isolated. The co-infection of VHH-pHEN-1-6xHis transfected TG1 *E. coli* strain with the M13KO7 helper phage was performed in the phage rescuing strategy, a total of 8×10^6 phage particles were obtained. To carry out the selection of anti-BthTX-I and BthTX-II VHHs, the phage displayed VHH library was submitted separately for immobilized BthTX-I or BthTX-II. After 1 round of panning against BthTX-I, 83 clones were selected. Of these, 82 clones presented the expected size for VHH by PCR colony. After 2 rounds against BthTX-II, 40 clones were grown on plates, and 28 were positive for VHHs. Once the presence of VHH in the colonies was confirmed, ELISA assays were performed to verify clone reactivity. Twenty-eight and six clones recognized BthTX-I and BthTX-II, respectively (Fig 1). It is important to note that 4 clones selected for BthTX-II were also able to recognize BthTX-I. However only 1 clone, selected for BthTX-I, showed cross-reactivity with BthTX-II. All clones that showed an absorbance value higher than the stipulated cut-off point (2 mean OD from negative samples plus 2 standard deviations) were considered positive.

Sequence analysis of anti-BthTX VHHs

After sequencing 34 ELISA positive clones, a multiple sequence alignment revealed 10 sequence profiles for BthTX-I, and 3 sequence profiles for BthTX-II, which were deposited in
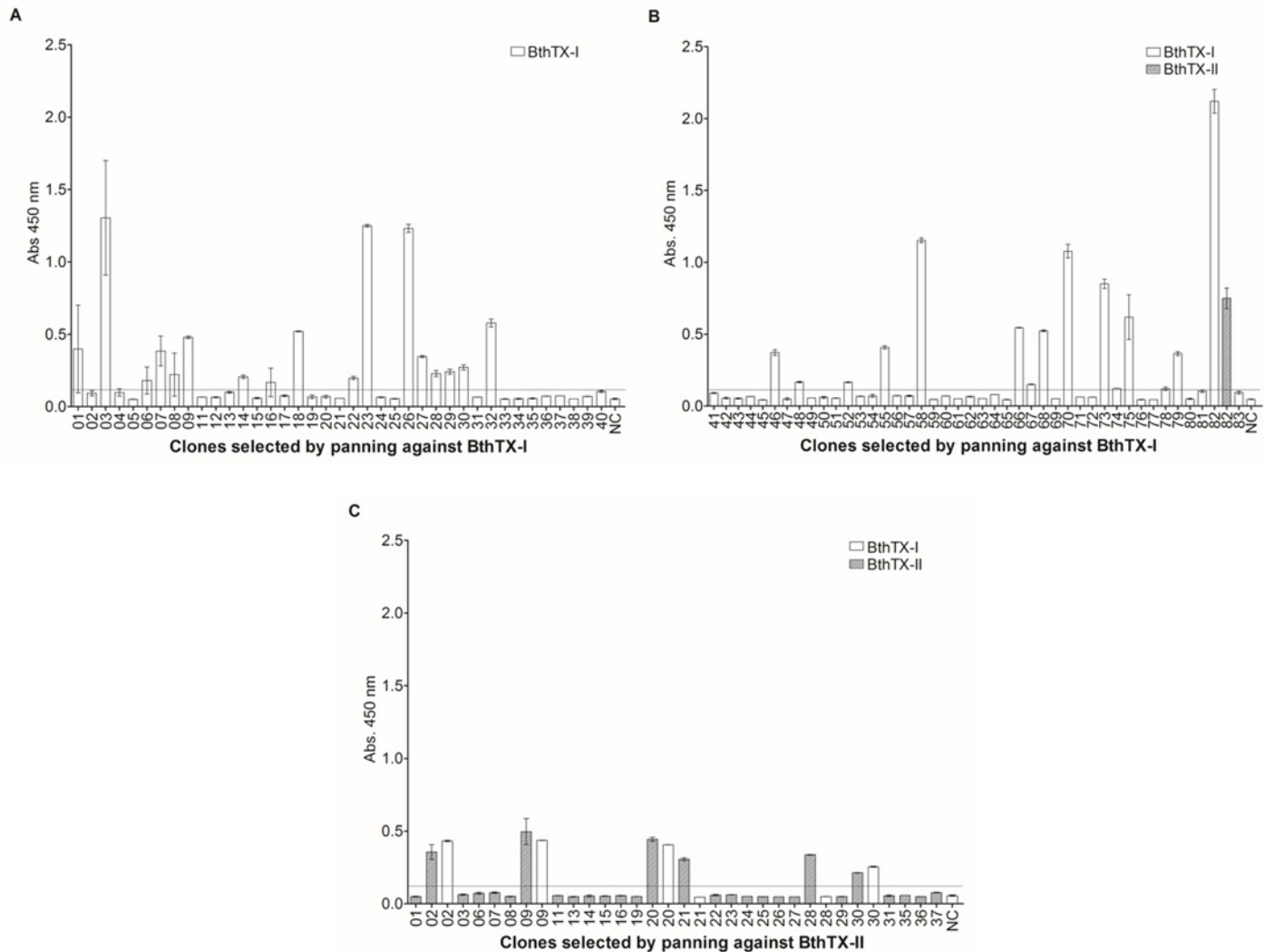
Fig 1. Selection of anti-BthTX-I and anti-BthTX-II VHHs. VHHs from the recombinant phage displayed library were submitted separately against immobilized BthTX-I or BthTX-II. After one round of panning, 82 and 28 clones selected for BthTX-I and BthTX-II, respectively, presented VHHs. ELISA assays were performed to verify clone reactivity. Twenty-eight (28) and six (06) clones recognized BthTX-I and BthTX-II. (A) Clonal reactivity of VHHs (1–40) selected against BthTX-I, NC–negative control; (B) Clonal reactivity of VHHs (41–83) selected against BthTX-I, Cross-reactivity of VHH 82 with BthTX-II, NC–negative control; (C) Clonal reactivity of VHHs (1–37) selected against BthTX-II, Cross-reactivity of 02, 09, 20, 21, 28 and 30 VHHs with BthTX-I, NC–negative control. All clones that showed an absorbance value (OD 450nm) higher than the stipulated cut-off point (2 mean OD from negative samples plus 2 standard deviations) were considered positive. All measurements were performed in triplicate. The negative control was performed using the llama pre-immune serum. Error bars represent standard deviation.

doi:10.1371/journal.pone.0151363.g001

the GenBank database under accession numbers: KC329709 (clone 9), KC329710 (clone 23), KC329711 (clone 32), KC329712 (clone 48), KC329713 (clone 58), KC329714 (clone 66), KC329715 (clone 67), KC329716 (clone 68), KC329717 (clone 75), KC329718 (clone 82), KF498607 (clone 20), KF498608 (clone 30) and KF498609 (clone 28), respectively. Based mainly on CDR homology and CDR3 length, 4 clusters of anti-BthTX VHHs (I-IV) were identified (Fig 2). The unique clone selected against BthTX-I (KC329718) that recognized BthTX-II showed a high similarity with members selected against BthTX-II. Cluster I is characterized by clones (KF498607, KF498608, KF498609, and KC329718) that presented a CDR3 length of 19 amino acid residues, with the consensus motif (S/T)ATYY(T/N)GEYYL(L/V)(Q/R)ADRYQH.

```
                    FR1                    CDR1          FR2              CDR2
KF498607  MAEVQLQASGGGLVQAGGSLRLSC  AASGRTFS  DLSMGWFRQAPGKEREFVA  AVSWSVGT ┐
KF498608  MAEVQLQASGGGLVQAGGSLRLSC  AASGRTFS  DLSMGWFRQAPGKEREFVA  AVSWSVGT │ I
KF498609  MAEVHLQASGGGLVQEGGSLRLSC  AASGRTFS  DLSMGWFRQAPGKEREFVA  AVSWTPGT │
KC329718  MAEVQLQASGGGLVQAGGSLRLSC  AASGGTFS  NPSMGWFRQAPGKEREFVA  AVSWSAGS ┘

KC329709  MAEVQLQASGGGLVQAGGSLRLSC  AASGPTYD  SYGMAWFRQGPGQGREFVA  AISLSHST ┐ II
KC329714  MADVQLQASGGGLVQAGGSLRLSC  AASGPIYE  SYGMAWFRQGPGQGREFVA  AIHLSSST ┘

KC329713  MAEVQLQASGGGLVQAGGSLRLSC  AASGRTDS  TYAMAWFRQAPGKEREFVA  AITYTGGT ┤ III

KC329710  MADVQLQASGGGLVQAGGSLRLSC  AASGNIDT  IDVMGWYRQAPGRQRELVA  DITSQG-S ┐
KC329711  MAEVQLQASGGGLVQAGGSLGLSC  AASGNIDT  IDVMGWYRQAPGKQRELVA  DITSQG-S │
KC329712  MADVQLQASGGGLVQAGGSLRLSC  AASGNINT  IDVMGWYRQAPGKQRELVA  DITRLA-S │ IV
KC329715  MAEVQLQASGGGLVQAGGSLRLSC  AASGNINT  IDVMGWYRQAPGKQRELVA  DITRLA-S │
KC329716  MAEVQLQASGGGLVQAGGSLRLSC  AASGNIDT  IDVMGWYRQAPGKQRELVA  DITSQG-S │
KC329717  MADVQLQASGGGLVQAGGSLRLSC  AASGNIDT  IDVMGWYRQAPGKQRELVA  DITSQG-S ┘
          **:*:*********** **** *** ****     *.*:**.**: **:**   :      :


                      FR3                          CDR3              FR4
KF498607  TYYADSVKGRFTISRDNAKNTVDLQMISLKPEDTAVYYC  SATYYTGEYYLLQADRYQH  WGQGTQVTVTVSS ┐
KF498608  TYYADSVKGRFTISRDNAKNTVDLQMISLKPEDTAVYYC  SATYYTGEYYLVQADRYQH  WGQ---VTVTVSS │ I
KF498609  TYYADSVKGRFTISRDNAKNTVDLQMISLKPEDTAVYYC  TATYYTGEYYLVQADRYQH  WGQGTQVTVTVSS │
KC329718  TYYADSVKGRFTISRDNAKNTVDLRMTSLKPEDTAVYYC  SATYYNGEYYLLRADRYQH  WGQGTQVTVTVSS ┘

KC329709  TYYADSVKGRFTISRGNAENTVYLQMNSLKPEDTAVYTC  AIGNLRIAVPPSSVG-YDY  WGQGTQVTVTVSS ┐ II
KC329714  TYYGDSVKGRFTISRDNAQNMVYLQMNSLKPEDTAIYFC  AIGNLRIAVPPTSVG-YDY  WGQGTQVTVTVSS ┘

KC329713  THYADSVKGRFTISRDVAKDIMYLQMNSLKPEDTAVYYC  AEKRSS-WYRPFGVDEFGS  WGQGTQVTVTVSS ┤ III

KC329710  TNYADSVKGRFTISRDNAKNTVYLQMNNLEPEDTAVYYC  AQWILSTDHSY-----KHY  WGQGTQVTVTVSS ┐
KC329711  TNYADSVKGRFTISRDNAKNTVYLQMNNLEPEDTAVYYC  AQWILSTDHSY-----KHY  WGQGTQVTVTVSS │
KC329712  ANYADSVKGRFTISRDNAKNTVYLQMNNLEPKDTAVYYC  AQWILSTDHSY-----MHY  WGQGTQVTVTVSS │ IV
KC329715  ANYADSVKGRFTISRDNAKNTVYLQMNNLEPKDTAVYYC  AQWILSTDHSY-----MHY  WGQGTQVTVTVSS │
KC329716  TNYADSVKGRFTISRDNAKNTVYLQMNNLEPEDTAVYYC  AQWILSTDHSY-----KHY  WGQGTQVTVTVSS │
KC329717  TNYADSVKGRFTISRDNAKNTVYLQMNNLEPEDTAVYYC  AQWILSTDHSY-----KHY  WGQGTQVTVTVSS ┘
          : *.**********. *:: : *:* .*:*:***:* *   :               *** * ..:
```

Fig 2. Amino acid sequence alignment of anti-BthTX-I and BthTX-II VHHs. The clones were clustered in four groups based on sequence homologies. The framework regions (FR) as well as the complementarity determining regions (CDR) are indicated with arrows; two conserved cysteines are shaded; VHH hallmark substitutions in FR2 and FR4 are bolded and underlined. Cluster I (KF498607, KF498608, KF498609, and KC329718), Cluster II (KC329709, KC329714), Cluster III (KC329713), and Cluster IV (KC329710, KC329711, KC329712, KC329715, KC329716, KC329717). The colon (:) represents highly conserved amino acids; the asterisk (*) represents identical amino acid residues; the period (.) means somewhat similar but different amino acids and blank represents dissimilar amino acids or gaps.

doi:10.1371/journal.pone.0151363.g002

Additionally, the 4 sequences showed well-conserved CDR1 and CDR2 (consensus motif: AASG(R/G)TFS, and AVSW(S/T)(V/P/A)G(T/S), respectively). Clones that constitute Cluster II (KC329709, KC329714) and III (KC329713) also showed a long CDR3, with 18 amino acid residues. In contrast, Cluster IV, represented by 6 members (KC329710, KC329711, KC329712, KC329715, KC329716, KC329717), possess a shorter CDR3 region with a conserved motif of 14 amino acid residues (AQWILSTDHSYKHY). Moreover, CDR1 and CDR2 share highly conserved consensus sequence motifs: AASGNI(D/N)T and DIT(S/R)(Q/L)(G/A)

S, respectively. Two conserved cysteine residues that form the canonical cross-species disulfide bond between FR1 and FR3, as well as the established hallmark amino acids in FR2 (Y/F37, E/Q44, R45, L/F47) that differentiate VHHs from conventional VHs were identified in the sequences. Only members of Cluster II did not present all 4 amino acid substitutions in FR2. Due to the high similarity observed between clones of Cluster I, and the great ability to recognize both proteins by ELISA, two clones KF498607 and KF498608, as well as the clone KC329718, selected during the panning for BthTX-I, were selected for futher experiments. Additionally, clone KC329715 belonging to Cluster IV, able to recognize only BthTX-I, was also investigated. After expressing VHHs (KF498607, KF498608, KC329718, KC329715) in the E. coli HB2151 strain, clones were purified by IMAC. Depending on the VHH clone, about 1 to 6 mg of recombinant protein per liter was obtained in culture flasks.

Western blot and interaction analysis by SPR

Clones KF498607, KF498608, and KC329718 were able to bind to BthTX-I and BthTX-II, used for VHH library construction. On the other hand, KC329715 showed no or weak interaction with the toxins. Pre-immune serum was not capable of recognizing the toxins in WB (Fig 3).

The affinity between CM5-BthTX-I and CM5-BthTX-II against selected purified VHHs (KC329718, KF498607, and KF498608) measured by SPR showed binding and dissociation sensograms, with which it possible to obtain the kinetic parameters using the 1:1 Langmuir model with highly reliable fit. This was evidenced by the low Chi^2 values obtained (< 1RU) (Table 2). All binding constants obtained were in the nanomolar range (10^{-7} to 10^{-9}). According to the kinetic model, KC329718 showed the highest affinity to BthTX-I, which has a K_D value (53.9 nM) eleven times lower than that obtained for KF498607 (628.7 nM) and KF498608 (668.1 nM). On the other hand, KF498607 VHH showed higher affinity to BthTX-II (K_D of 28.0 nM) than observed for KC329718 (770.2 nM) and KF498608 (42.7 nM) (Fig 4/Table 2).
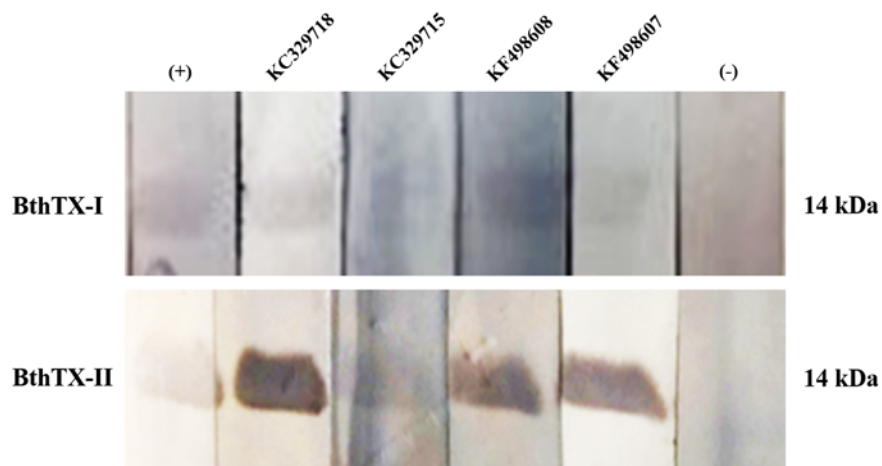
Fig 3. Western blot of purified VHHs against BthTX-I. 15% SDS-PAGE was carried out to resolve BthTX-I and BthTX-II under reducing conditions. After electrophoresis, BthTX-I and BthTX-II were electrotransferred to a nitrocellulose membrane and probed with selected VHHs (KF498607, KF498608, KC329715, and KC329718). Samples were incubated with mouse anti-His antibody followed by HRP-conjugated anti-mouse IgG produced in goat. Reactive signals were detected by DAB staining in the presence of hydrogen peroxide. *Lama glama* pre-immune serum was used as negative control (-), and *Lama glama* immune serum, as positive control (+).

doi:10.1371/journal.pone.0151363.g003

Table 2. Interaction analysis by SPR.

Immobilized antigen	VHH	k_{on} [1/Ms]	k_{off} [1/s]	R_{max} [RU]	K_D [M]	Chi2 [RU]
BthTX-I	KC329718	$6.417 \times 10^{+5}$	0.0346	185.0	5.387×10^{-8}	0.709
	KF498607	$2.574 \times 10^{+5}$	0.1618	1,188	6.287×10^{-7}	0.874
	KF498608	$1.786 \times 10^{+5}$	0.1193	1,110	6.681×10^{-7}	0.697
BthTX-II	KC329718	$3.347 \times 10^{+5}$	0.2578	18.4	7.702×10^{-7}	0.024
	KF498607	$1.839 \times 10^{+5}$	0.5157	60.6	2.800×10^{-8}	0.014
	KF498608	$7068 \times 10^{+5}$	0.0302	125.7	4.270×10^{-8}	0.101

Binding kinetics parameters were measured according to SPR sensorgrams shown in Fig 4 using the 1:1 Langmuir model.

doi:10.1371/journal.pone.0151363.t002

Inhibition of phospholipase activity by VHHs

The ability of phospholipase inhibition by VHHs was assayed using synthetic fluorescent phospholipid. As shown in Fig 5, all clones presented some degree of inhibition, except the clone KC329715. The best result was obtained by KC329718, which demonstrated an inhibition of up to 60% at a ratio of 1:40 (BthTX-II:VHH).
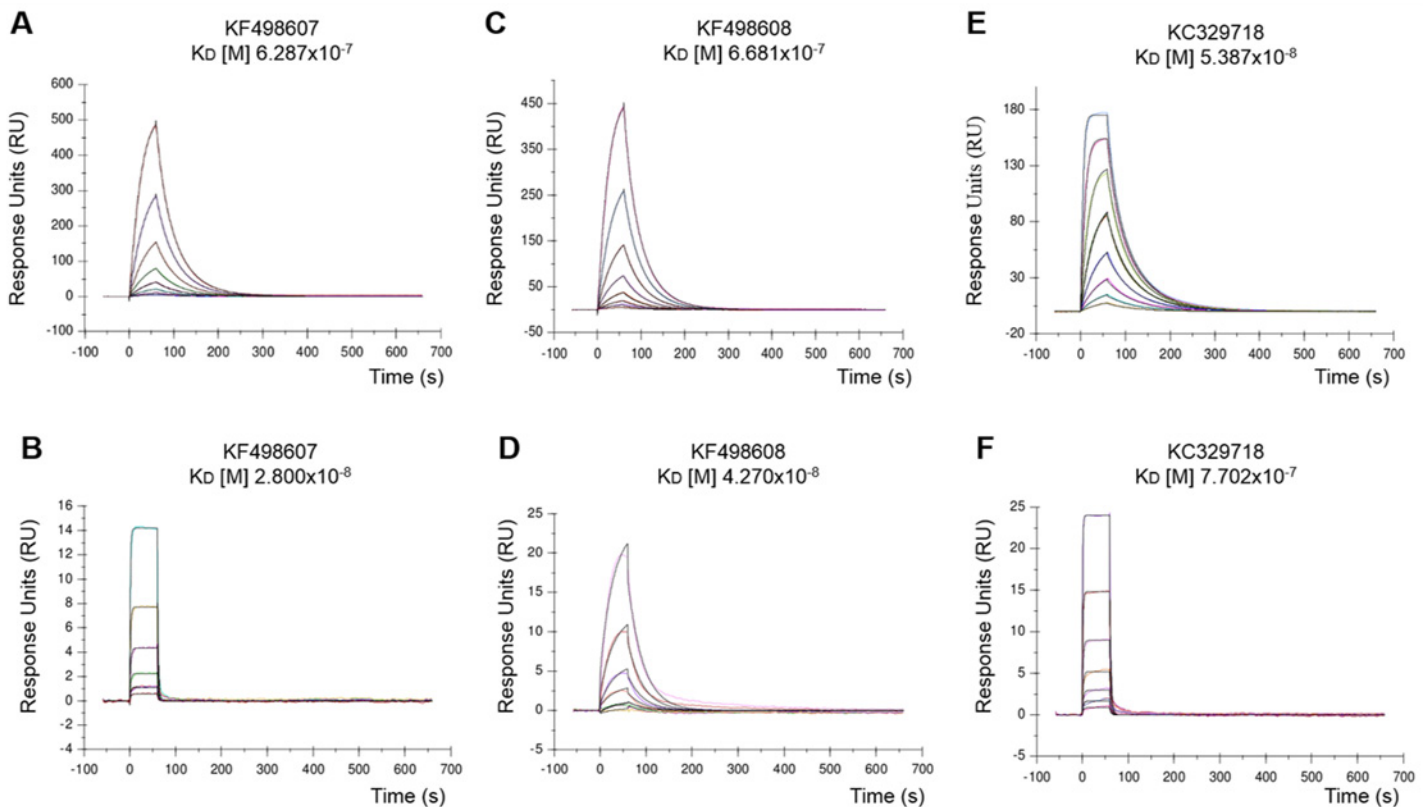
Fig 4. VHHs affinity to BthTX-I and BthTX-II. Representative sensorgrams of the interaction were measured in a Biacore T200 system (GE Healtcare). Purified VHHs (KF498607, KF498608 and KC329718) at concentrations of 6.25 to 0.049 µg/mL were flowed over a BthTX-I-coated CM5 chip and 25 to 0.006 µg/mL were used for immobilized BthTX-II. (A) KF498607 x BthTX-I; (B) KF498607 x BthTX-II; (C) KF498608 x BthTX-I; (D) KF498608 x BthTX-II; (E) KC329718 x BthTX-I; (F) KC329718 x BthTX-II. Assays were injected in a flow rate of 30 µl/min at 37°C. RU indicates resonance units.

doi:10.1371/journal.pone.0151363.g004
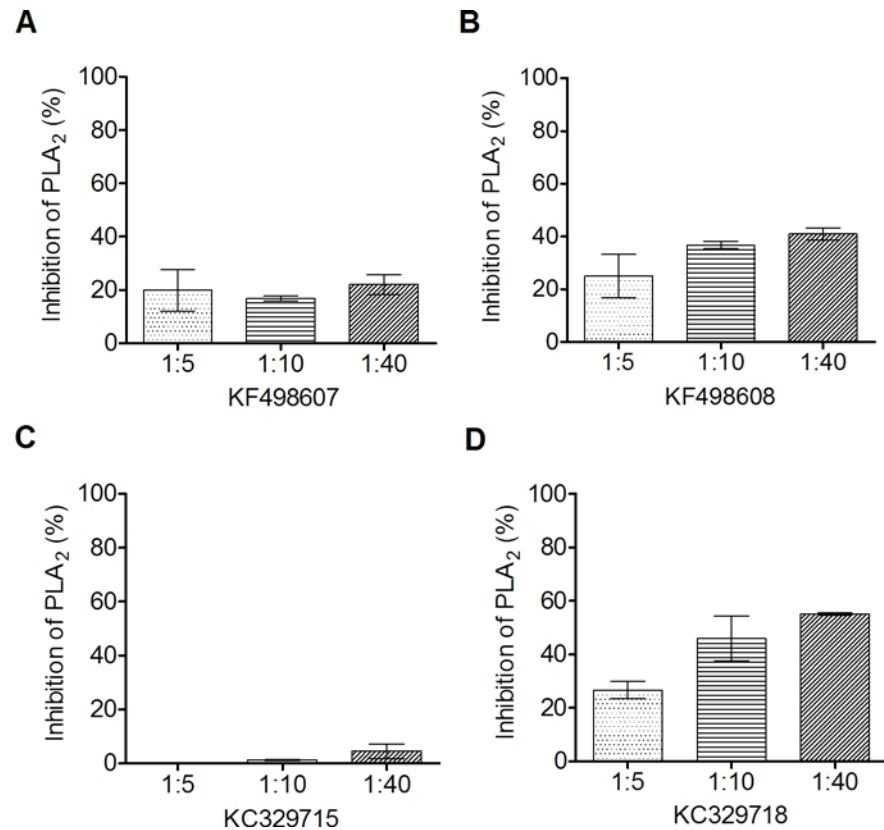
Fig 5. *In vitro* inhibition of phospholipase activity. The quantification of phospholipase activity inhibition by selected VHHs was assayed using synthetic fluorescent phospholipid. To verify the ability of VHHs to inhibit the phospholipase activity of BthTX-II, the toxin was pre-incubated with selected VHHs for 30 minutes at 37°C in different proportions (1:5; 1:10 and 1:40 w/w). Inhibition of phospholipase activity by (A) KF498607; (B) KF498608; (C) KF329715; (D) KC329718. BthTX-II activity on the phospholipid, in the absence of VHH, was used as a positive control, and considered as having 100% activity. The negative controls were carried out using medium reaction without BthTX-II. All measurements were performed in duplicate. Error bars represent standard deviation.

doi:10.1371/journal.pone.0151363.g005

Cross reactivity of anti-BthTX VHHs and myotoxicity neutralization

KF498607, KF498608, KC329715 and KC329718 selected for cross reacivity showed interactions, at different levels, with the majority of venoms and PLA$_2$s from different species of the *Bothrops* genus. On the other hand, the clones presented no reaction with venoms or toxins isolated from other members of the Viperidae or Elapidae families, indicating genus specificity ([Fig 6](#)). Myotoxicity induced by *B. jararacussu* venom, BthTX-I and BthTX-II was determined by CK activity. In a proportion of 1:5 (w/w), 10 μg BthTX-I or venom to 50 μg VHH, and 15 μg BthTX-II to 75 μg VHH, KF498607 was capable of inhibiting about 75% of the myotoxicity induced by BthTX-I, BthTX-II and venom. In the same proportion, KC329718 inhibited about 48% and 56% of BthTX-I and BthTX-II-induced myotoxicity, respectively, but showed no significant venom inhibition. However, when the assay was performed increasing the proportion to 1:10 (w/w) of venom:VHH, KC329718 presented about 73% of myotoxicity inhibition. Furthermore, when the capacity of both clones to inhibit MTX-I was analyzed, VHHs were able to neutralize around 50–55% of toxin activity ([Fig 7](#)).
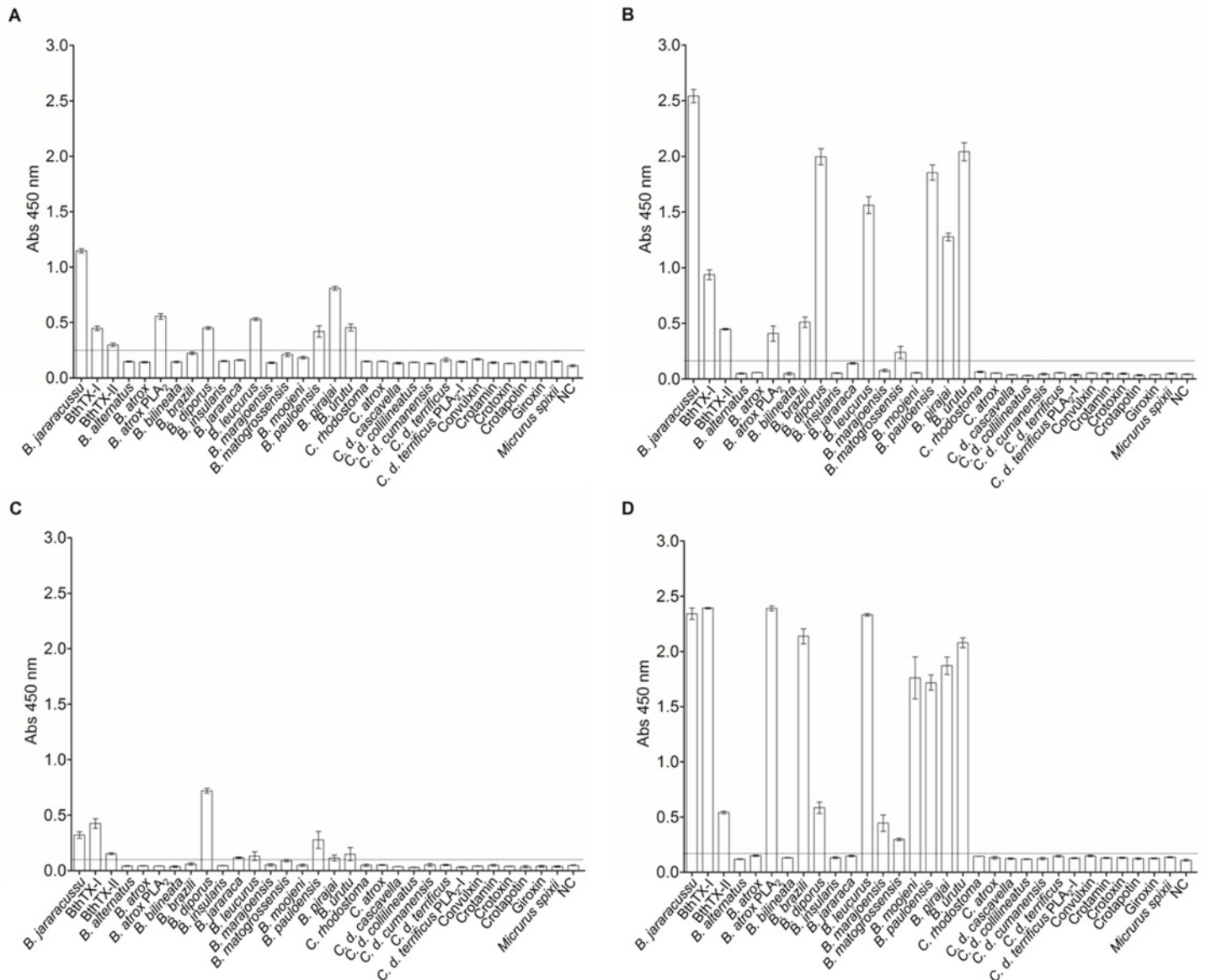
Fig 6. Cross-reactivity of anti-BthTX-I and BthTX-II VHHs. *In vitro* reactivity showing different levels of interaction of selected VHHs (A) KF498607; (B) KF498608; (C) KF329715; (D) KC329718 with a variety of snake venoms (*Bothrops alternatus*, *Bothrops atrox*, *Bothrops bilineata*, *Bothrops brazili*, *Bothrops diporus*, *Bothrops insularis*, *Bothrops jararaca*, *Bothrops leucurus*, *Bothrops marajoensis*, *Bothrops matogrossensis*, *Bothrops moojeni*, *Bothrops pauloensis*, *Bothrops pirajai*, *Bothrops urutu*, *Calloselasma rhodostoma*, *Crotalus atrox*, *Crotalus durissus cascavella*, *Crotalus durissus collilineatus*, *Crotalus durissus cumanensis*, *Crotalus durissus terrificus*, *Micrurus spixii*), and isolated toxins (PLA$_2$ from *Bothrops atrox*, and PLA$_2$-I, convulxin, crotamin crotapotin, and crotoxin, and giroxin from *Crotalus durissus terrificus*). After being coated on the wells, venoms and toxins were probed with selected VHHs. Samples were incubated with mouse anti-His antibody and the reactive signals were detected after incubation with HRP-conjugated anti-mouse IgG produced in goat and TMB. All clones that showed an absorbance value (OD 450nm) higher than the stipulated cut-off point (2 mean OD from negative samples plus 2 standard deviations) were considered positive. The dashed lines represent the cut off. All measurements were performed in triplicate. For the negative control (NC), wells were not coated with venoms or toxins. Error bars represent standard deviation.

doi:10.1371/journal.pone.0151363.g006

Modelling and interface binding of the VHHs and BthTX-I and BthTX-II

A BLAST search revealed 3 putative templates of high-level similarity with the target sequences (KF498607, KF498608, KC329715 and KC329718), as shown in Table 3. The percentage of residues lying in the favored regions of a Ramachandran plot [37] is one of the best guides to
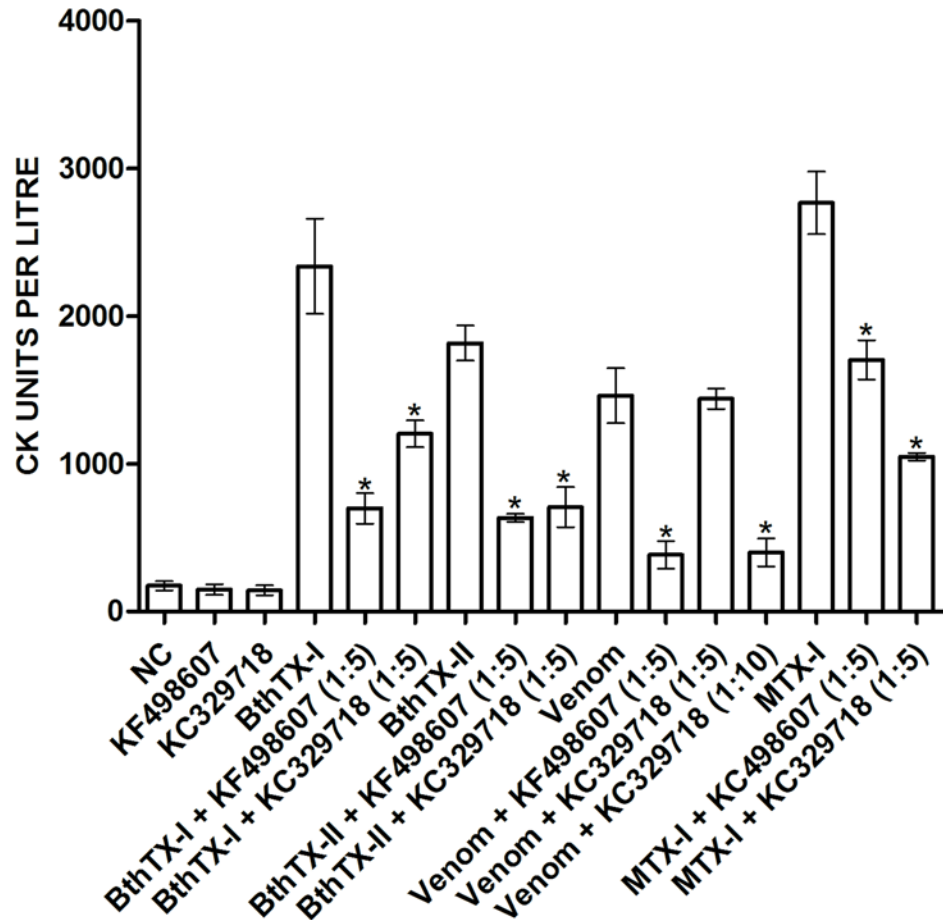
Fig 7. *In vivo* neutralization of *B. jararacussu* venom and PLA$_2$-induced myotoxicity by VHHs. Plasma creatine kinase (CK) levels were measured at 340 nm to determine VHH ability to inhibit the myotoxicity caused by *B. jararacussu* venom or PLA$_2$s, or by a related toxin, MTX-I, a PLA$_2$ isolated from *B. brazili*. For this, groups of 5 animals were injected with PBS, VHH KF498607, VHH KC329718, BthTX-I, BthTX-I + VHH KF498607, BthTX-I + VHH KC329718, BthTX-II, BthTX-II + VHH KF498607, BthTX-II + VHH KC329718, *B. jararacussu* venom, *B. jararacussu* venom + VHH KF498607, *B. jararacussu* venom + VHH KC329718, MTX-I, MTX-I + VHH KC329718, MTX-I + VHH KC329718. Before administration to mice, venom or PLA$_2$s and antibody preparations were pre-incubated at 37°C for 1 h, in a proportion 1:5 or 1:10 (w/w). The negative control was performed with PBS or VHHs, and as a positive control, animals were injected with *B. jararacussu* venom, BthTX-I, BthTX-II or MTX-I without the addition of VHH. Bonferroni's test was used for significance analysis. (*) P <0.05. Error bars represent standard deviation.

doi:10.1371/journal.pone.0151363.g007

checking the stereochemical quality of a protein model. Based on the assumption that a good model should have more than 90% of the amino acid residues in the allowed regions [29], the Ramachandran plot analysis for all VHH structures indicated more than 90.04% of amino acid

Table 3. PDB code, resolution, references, percent similarity and RMSD of templates for modeled VHHs.

Target (VHH clone)	Template (PDB:chain)	% Identity	Resolution (Å)	RMSD (Å)	Reference Template
KF498607	4KRP:B	72.73	2.82	0.38	Schmitz, K.R., 2013
KF498608	4DKA:A	72.87	1.97	0.52	Park, Y.J., 2012
KC329715	3EZJ:B	70.97	2.80	0.45	Korotkov, K.V., 2009
KC329718	4KRP:B	73.85	2.82	0.33	Schmitz, K.R., 2013

doi:10.1371/journal.pone.0151363.t003

residues in favorable regions. The model quality was also assessed by comparing the predicted structure with the template via superimposition and atoms RMS deviation (RMSD) assessment. The RMSD of $C\alpha$ trace between all homology structures and templates is less than 1.00 Å, supporting the idea that the generated models are reasonably good and quite similar to the templates (Table 3). The best dimeric interactions between VHHs (KF498607 and KC329718) and BthTX-I and BthTX-II, presenting the lowest ClusPro scores, are represented in Fig 8. Table 4 shows the hydrogen bonds formed between VHHs and toxins in the final docking model for KF498607 and KC329718. While results for KF498608 were quite similar to KF498607, the KC329715 VHH showed no good interaction with BthTX-I and BthTX-II.
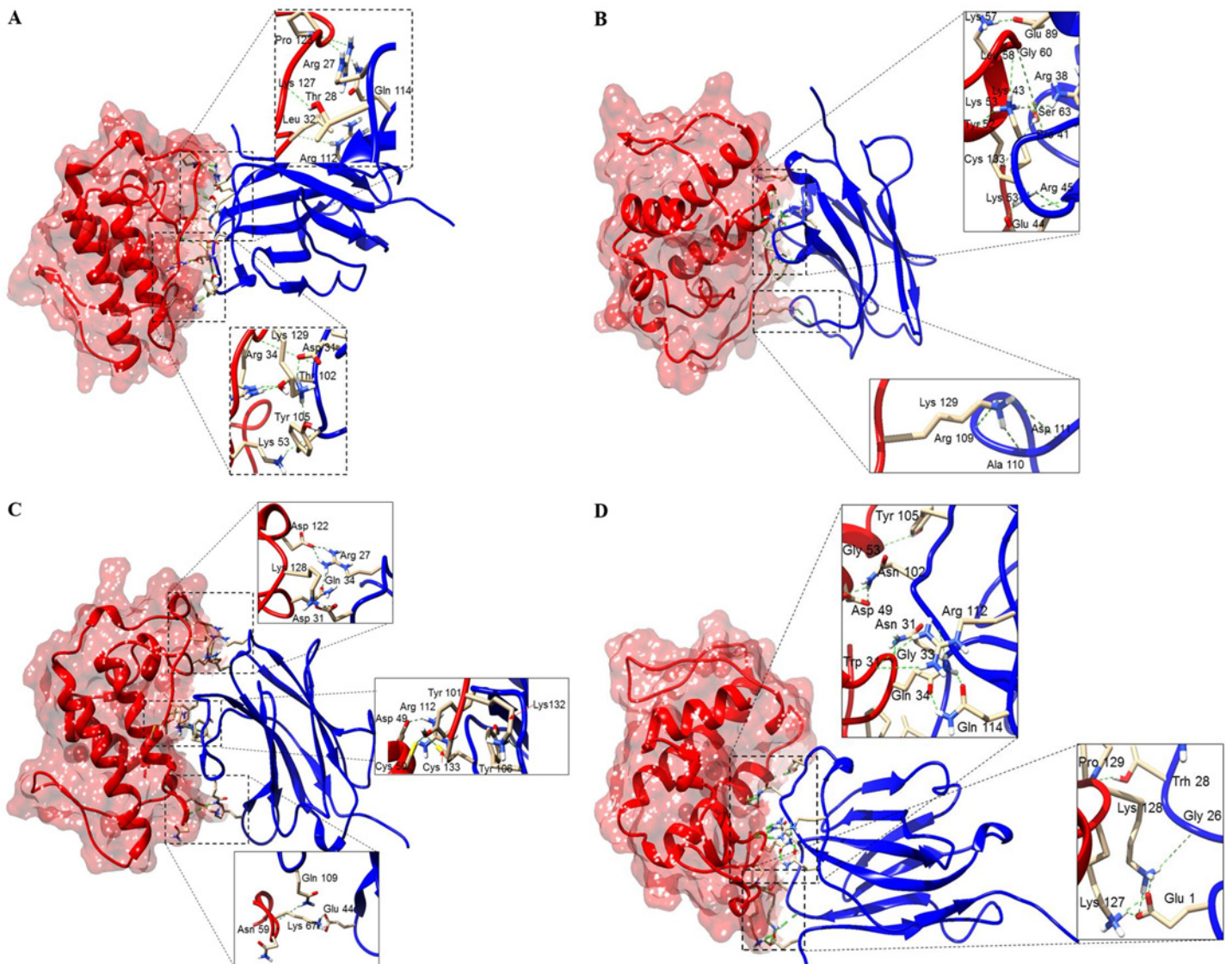
Fig 8. Docking results showing binding sites of VHHs on surfaces of PLA₂s. (A) KF498607 (blue ribbon) and BthTX-I (red surface); (B) KC329718 (blue ribbon) and BthTX-I (red surface); (C) KF498607 (blue ribbon) and BthTX-II (orange surface); (D) KC329718 (blue ribbon) and BthTX-II (orange surface). The interaction sites were enlarged to show hydrogen bonds formed between the amino acid residues. Both VHHs covered the enzymatic groove surface areas of the modeled BthTX-II and inserted the CDR3 into the catalytic cleft, as well as being able to interact with amino acid residues of the PLA₂ C-termini.

doi:10.1371/journal.pone.0151363.g008

Table 4. Molecular interactions between the amino acid residues of VHHs and PLA$_2$s.

Clone	VHH	Amino acid residue		Toxin Domain	Antigen
	Domain	Antibody	Antigen		
KF498607	CDR1	Arg27	Pro123	C-terminal	BthTX-I
	CDR3	Gln114	Pro123	C-terminal	
	CDR1	Thr28	Lys127	C-terminal	
	CDR3	Arg112	Leu32	Ca^{++}-binding site	
	FR2	Asp31	Lys129	C-terminal	
	CDR3	Thr102	Arg34	Ca^{++}-binding site	
	CDR3	Tyr105	Lys53	α-2 helix	
KC329718	FR3	Glu89	Lys57	α-2 helix	BthTX-I
	FR2	Arg38	Lys53	α-2 helix	
	FR2	Lys43	Leu58	α-2 helix	
	FR2	Lys43	Tyr52	α-2 helix	
	FR3	Ser63	Cys133	C-terminal	
	FR2	Pro41	Gly60	α-2 helix	
	FR2	Arg45	Lys53	α-2 helix	
	FR2	Glu44	Lys53	α-2 helix	
	CDR3	Asp111	Lys129	C-terminal	
	CDR3	Arg109	Lys129	C-terminal	
	CDR3	Ala110	Lys129	C-terminal	
KF498607	CDR1	Arg27	Asp122	C-terminal	BthTX-II
	CDR1	Arg27	Gln34	Ca^{++}-binding site	
	FR2	Asp31	Lys128	C-terminal	
	CDR3	Tyr101	Cys133	C-terminal	
	CDR3	Tyr101	Cys133	C-terminal	
	CDR3	Tyr106	Lys132	C-terminal	
	CDR3	Arg112	Asp49	Catalytic site	
	CDR3	Gln109	Asn59	α-2 helix	
	FR2	Glu44	Lys67	α-2 helix	
KC329718	CDR3	Tyr105	Gly53	α-2 helix	BthTX-II
	CDR3	Asn102	Asp49	Catalytic site	
	CDR3	Arg112	Trp31	Catalytic site	
	FR2	Asn31	Gly33	Ca^{++}-binding site	
	CDR3	Gln114	Gln34	Ca^{++}-binding site	
	CDR1	Thr28	Pro129	C-terminal	
	CDR1	Gly26	Lys128	C-terminal	
	FR1	Glu1	Lys128	C-terminal	
	FR1	Glu1	Lys127	C-terminal	

doi:10.1371/journal.pone.0151363.t004

Discussion

Over the years, antivenom production has taken advantage of technological improvements in antigen preparation, immunization strategies, antibody fragmentation, as well as in the purification and preservation of antivenoms. These approaches have ensured advances in terms of activity, stability and antivenom safety, especially with regard to the hypersensitivity reactions and to the risk of zoonosis transmission [38,39]. Although antivenoms prevent or reverse most of the effects observed in snakebite victims, minimizing the mortality and physical sequelae

occasioned by the envenoming, the inhibition of local tissue damage remains the major challenge for antivenom therapy [39].

Through advances in antibody engineering, monoclonal antibody fragments, which are able to quickly reach dense tissues and stop the progress of local damages, have been selected against venom relevant epitopes [10,14]. In this way, we selected VHHs against BthTX-I and BthTX-II from *B. jararacussu* venom.

Considering that PLA$_2$s, frequently abundant in snake venoms from the Viperidae family [40], contribute substantially to local myotoxicity, anti-BthTX VHHs could limit the tissue necrosis and sequelae induced by bothropic envenoming.

To identify anti-BthTX VHHs, we produced an immune VHH library after the immunization of a *Lama glama* with purified BthTX-I and BthTX-II. Following a protocol based on "low dose, low volume, multi-site immunization" described by [41], with modifications in terms of adjuvant usage, injection volumes, and intervals between the immunizations, the animal generated a satisfatory immune response to both toxins. The high antiserum titre exhibited for BthTX-I and BthTX-II at the end of the immunization schedule is comparable to studies that used snake venoms to immunize camelids [14]. Furthermore, the animal did not present visible signs of local myotoxicity at the injections sites, despite simultaneous administration of both toxins.

With $>10^7$ individual clones, the generated library seemed to ensure a high diversity of the llama VHH gene repertoire [42]. Besides that, after the construction of a phage-displayed VHH library and 1 round of biopanning for BthTX-I and 2 rounds for BthTX-II, VHH inserts were detected in 99% and 70% of the selected phagemids, respectively. Inspired by the work of [43], in which with a unique round of panning, VHHs able to inhibit the enzymatic activity of the Botulinum toxin in a nanomolar range were selected, the individual clones were analyzed by ELISA and the sequencing of positive clones were performed.

Despite a high similarity (about 70%) between BthTX-I and BthTX-II [20], indirect ELISA revealed that only 1 clone was able to interact with BthTX-II. On the other hand, 4 clones selected against BthTX-II presented cross reactivity with BthTX-I, indicating that these VHHs would interact with similar epitopes of both toxins and may even originate from the same B-cell lineages.

Sequence analysis showed that the clones selected against BthTX-I and BthTX-II presented the VHH hallmarks in 13 different profiles. The amino acid substitutions reshape the side that interacts with the VL domain, preventing the binding to the light chain. Besides that, these substitutions promote an increase in VHH solubility and thermostability [44,45]. According to [14], VHHs based on the high CDR sequence identity and CDR3 length were grouped. All 4 clusters presented a CDR3 containing between 14 and 19 amino acid residues, which could enable its insertion into sites not usually accessible to conventional antibodies [16]. The unique clone (KC329718) selected against BthTX-I that recognized both proteins showed about 90% identity with clones selected against BthTX-II, reinforcing the idea that these VHHs interact with common antigenic sites of the proteins.

In order to verify VHH ability to specifically recognize the PLA$_2$, Western Blot analysis was performed. While *L. glama* post-immune serum and KF498607, KF498608, KC329718 VHHs were able to detect the reduced proteins in different degrees of reactivity, KC329715 VHH presented weak or no interaction with BthTX-I and BthTX-II, respectively. This is probably due to the difference in affinity between the clones.

Therefore, an SPR assay was used to evaluate the kinetic interactions between the selected VHHs and BthTX-I and BthTX-II. When compared with other anti-BthTX VHHs, the KC329718 VHH showed the highest affinity for BthTX–I (K$_D$ 53.8 nM), similar to K$_D$ values

obtained by VHH selected against AahI, a neurotoxin from *Androctonus australis hector* scorpion, that was able to neutralize the toxin activity in 100% of treated swiss mice [46].

Additionally, *in vitro* assays, performed to investigate the ability of selected VHHs to inhibit the phospholipase activity of BthTX-II, demonstrated that 3 clones were capable of reducing this activity by up to 60%. Despite molar excess of VHHs over toxin does not improve PLA$_2$ inhibition significantly, the data suggest that these VHHs could interact with amino acid residues of the toxin enzymatic cleft, as described by [47].

Moreover, the clones presented cross reactivity with PLA$_2$s or venoms from different *Bothrops* species, indicating specificity and that VHHs react with similar antigenic sites of orthologous proteins, important features for snakebite diagnostic or serumtherapy [48,49]. It is important to note that in all *in vitro* experiments, the KC329715 VHH demonstrated lower or no reactivity against the tested venoms and toxins. This may possibily be due to smaller CDR2 and CDR3, observed among the members of cluster IV (Fig 2).

In *in vivo* assays carried out with KC329718 and KF498607 VHHs clearly demonstrated a significant decrease in mice serum CK levels, inoculated with BthTX-I, BthTX-II or *B. jararacussu* venom. A higher concentration of KC329718 enhanced its inhibitory effect upon BthTX-I, BthTX-II and venom-induced myotoxicity. Although 5-fold molar excess over toxins, selected VHHs were not able to abolish the myotoxicity induced by the PLA$_2$s and venom, as observed in the neutralization of *B. asper* myotoxins using murine monoclonal antibody at a 1:1 molar ratio [50]. Despite having a 12-fold greater affinity for BthTX-I and showing higher ability to inhibit *in vitro* PLA$_2$ activity of BthTX-II, the clone KC329718 seems to present lower ability to neutralize *in vivo* myotoxicity induced by *B.jararacussu* venom or BthTX-I. This probably occurs due to the differences between epitope specificity indicated in the molecular docking (Table 4).

In addition, the *in vivo* results confirmed the cross-reactivity of the ELISA tests, when both clones were able to inhibit MTX-I activity. Given that several studies show antivenom cross neutralization activity on specific venom toxicities of heterologous species in animal studies [49,51], our data points to the VHH's relevance in the neutralization and cross neutralization of local damages caused by *Bothrops* venom. However, both specificity and high affinity are critical parameters of antibodies for therapeutic utility. Thus, protein engineering and mutagenesis strategies could be used for the enhancement of VHH affinity.

Previous studies indicate that myotoxic PLA$_2$s target the sarcolemma as their primary site of action, which leads to a prominent influx of calcium ions and an efflux of potassium and ATP, besides other intracellular markers, inducing an acute degeneration of skeletal muscle fibers [52–54]. To trigger these events, these PLA$_2$s can act by two mechanisms: i. hydrolysis of glycerophospholipids at the sn-2 position of the glycerol backbone, releasing fatty acids and lysophospholipids, a mechanism depending on Ca^{++} [47]; ii. direct cytolysis, in cases of proteins that show either no, or low catalytic activity [55]. This mechanism involves an allosteric transition and two independent interaction sites with the target membrane, i.e., cationic membrane docking site (MDoS), and hydrophobic membrane-disruption site (MDiS) [53].

Molecular docking suggested that KC329718 and KF498607 VHHs, members of Cluster I, bound to amino acid residues of the toxin C-termini, which may constitute putative MDoS of BthTX-I and BthTX-II, as suggested by [53], avoiding the protein-membrane docking. When compared with further clusters, the presence of conserved amino acid residues into VHH CDR3 (Ala110, Asp111, Arg112, Gln114) could significantly influence the interaction between VHHs and both toxins (Fig 2/Table 4). Besides that, both ligands seem to bind the Asp49 residue of BthTX-II's enzymatic cleft, inhibiting the binding of Ca^{++}, essential to its catalytic activity [47]. The formation of a hydrogen bond between Arg112 of KC329718 and Trp31 of BthTX-II may contribute to the decrease of the toxin's phospholipase activity, as shown in Fig

5, since this amino acid residue also participates in the catalytic reaction [56]. Co-crystallization assays are being performed in order to confirm the results and to understand the myotoxic mechanism of both proteins.

Taken together, selected VHHs are able to recognize specifically BthTX-I and BthTX-II as well as to decrease the myotoxicity of *Bothrops jararacussu* venom. This inhibition is directly related to VHH insertion in the catalytic cleft and interaction with the C-termini of these phospholipases, essential for myotoxic activity. Therefore, these clones could represent a convenient tool for investigating action mechanisms of toxins, bioprospection, the development of alternative methods to snakebite diagnosis, and even as therapeutic agents to overcome the challenges of the current serumtherapy.

Acknowledgments

Author Contributions

Conceived and designed the experiments: CFCF RGS AMS JPZ FBZ LHPS. Performed the experiments: NDRP SSP MPS MSSM AMK LSMD MBL FBZ CFF MEFH. Analyzed the data: NDRP SSP CFCF LSMD FBZ LAC ALF AMS RGS. Contributed reagents/materials/analysis tools: RGS CFCF AMS ALF LAC JPZ LHPS. Wrote the paper: CFCF NDRP JPZ.

References

1. Chippaux JP. Snake-bites: Appraisal of the global situation. Bull World Health Organ. 1998; 76: 515–524. PMID: 9868843

2. Kasturiratne A, Wickremasinghe AR, De Silva N, Gunawardena NK, Pathmeswaran A, Premaratna R, et al. The global burden of snakebite: a literature analysis and modelling based on regional estimates of envenoming and deaths. PLoS Med. 2008; 5: 1591–1604. doi: 10.1371/journal.pmed.0050218

3. World Health Organization. Snake antivenoms. 2015. Available: http://www.who.int/mediacentre/factsheets/fs337/en/. Accessed 20 March 2015.

4. Hansson E, Sasa M, Mattisson K, Robles A, Gutiérrez JM. Using geographical information systems to identify populations in need of improved accessibility to antivenom treatment for snakebite envenoming in Costa Rica. PLoS Negl Trop Dis. 2013; 7: 1–13. doi: 10.1371/journal.pntd.0002009

5. Otten EJ. Venomous animal injuries. In: Marx J, Hockberger R, Walls R, editors. Rosen's emergency medicine—concepts and clinical practice. Amsterdam: Eselvier; 2013. pp. 794–807.

6. Gutiérrez JM, Theakston RDG, Warrell DA. Confronting the neglected problem of snake bite envenoming: the need for a global partnership. PLoS Med. 2006; 3: 0727–0731. doi: 10.1371/journal.pmed.0030150

7. Dart RC, Sullivan JB Jr. Crotaline snake envenomation. In: Wolfson AB, Hendey GW, Ling LJ, Rosen CL, Schaider JJ, Sharieff GQ, editors. Clinical practice of emergency medicine. Philadelphia: Wolters Kluwer Health; 2005. pp. 1624–1626.

8. Cardoso DF, Yamaguchi IK, Silva AMM. Produção de soros antitoxinas e perspectivas de modernização por técnicas de biologia molecular. In: Cardoso JLC, França FOS, Wen FH, editors. Animais peçonhentos no Brasil: biologia, clínica e terapêutica dos acidentes. São Paulo: Sarvier; 2009. pp 419–431.

9. Gutierrez JM, Léon G, Lomonte B. Pharmacokinetic-pharmacodynamic relationships of immunoglobulin therapy for envenomation. Clin Pharmacokinet. 2003; 42: 721–741. doi: 10.2165/00003088-200342080-00002 PMID: 12846594

10. Cardoso DF, Nato F, England P, Ferreira ML, Vaughan TJ, Mota I, et al. Neutralizing human anti crotoxin scFv isolated from a nonimmunized phage library. Scand J Immunol. 2000; 51: 337–344. doi: 10.1046/j.1365-3083.2000.00709.x PMID: 10736105

11. Fernandes I, Assumpção GG, Silveira CRF, Faquim-Mauro EL, Tanjoni I, Carmona AK, et al. Immunochemical and biological characterization of monoclonal antibodies against BaP1, a metalloproteinase from *Bothrops asper* snake venom. Toxicon. 2010; 56: 1059–1065. doi: 10.1016/j.toxicon.2010.07.014 PMID: 20674587

12. Mousli M, Devaux C, Rochat H, Goyffon M, Billiald P. A recombinant single-chain antibody fragment that neutralizes toxin II from the venom of the scorpion *Androctonus australis hector*. FEBS Lett. 1999; 442: 183–188. doi:S0014-5793(98)01647-0 PMID: 9928998

13. Chames P, Van Regenmortel M, Weiss E, Baty D. Therapeutic antibodies: successes, limitations and hopes for the future. Br J Pharmacol. 2009; 157: 220–233. doi: 10.1111/j.1476-5381.2009.00190.x PMID: 19459844

14. Richard G, Meyers AJ, McLean MD, Arbabi-Ghahroudi M, MacKenzie R, Hall JC. *In vivo* neutralization of α-cobratoxin with high-affinity llama single-domain antibodies (VHHs) and a VHH-Fc antibody. PLoS One. 2013; 8: e69495. doi: 10.1371/journal.pone.0069495 PMID: 23894495

15. Helma J, Cardoso MC, Muyldermans S, Leonhardt H. Nanobodies and recombinant binders in cell biology. J Cell Biol. 2015; 209: 633–644. doi: 10.1083/jcb.201409074 PMID: 26056137

16. De Genst E, Silence K, Decanniere K, Conrath K, Loris R, Kinne J, et al. Molecular basis for the preferential cleft recognition by dromedary heavy-chain antibodies. Proc Natl Acad Sci USA. 2006; 103: 4586–4591. doi: 10.1073/pnas.0505379103 PMID: 16537393

17. Lauwereys M, Ghahroudi MA, Desmyter A, Kinne J, Hölzer W, De Genst E, et al. Potent enzyme inhibitors derived from dromedary heavy-chain antibodies. EMBO J. 1998; 17: 3512–3520. doi: 10.1093/emboj/17.13.3512 PMID: 9649422

18. Hassanzadeh-Ghassabeh G, Devoogdt N, De Pauw P, Vincke C, Muyldermans S. Nanobodies and their potential applications. Nanomedicine (Lond). 2013; 8: 1013–1026. doi: 10.2217/nnm.13.86

19. Andrião-Escarso SH, Soares AM, Rodrigues VM, Angulo Y, Díaz C, Lomonte B, et al. Myotoxic phospholipases A2 in *Bothrops* snake venoms: effect of chemical modifications on the enzymatic and pharmacological properties of bothropstoxins from *Bothrops jararacussu*. Biochimie. 2000; 82: 755–763. doi: 10.1016/S0300-9084(00)01150-0 PMID: 11018293

20. Kashima S, Roberto PG, Soares AM, Astolfi-Filho S, Pereira JO, Giuliati S, et al. Analysis of *Bothrops jararacussu* venomous gland transcriptome focusing on structural and functional aspects: I-gene expression profile of highly expressed phospholipases A2. Biochimie. 2004; 86: 211–219. doi: 10.1016/j.biochi.2004.02.002 PMID: 15134836

21. Pereira SS, Moreira-Dill LS, Morais MSS, Prado NDR, Barros ML, Koishi AC, et al. Novel camelid antibody fragments targeting recombinant nucleoprotein of Araucaria hantavirus: a prototype for an early diagnosis of Hantavirus Pulmonary Syndrome. PLoS One. 2014; 9: e108067. doi: 10.1371/journal.pone.0108067 PMID: 25243411

22. Ghahroudi MA, Desmyter A, Wyns L, Hamers R, Muyldermans S. Selection and identification of single domain antibody fragments from camel heavy-chain antibodies. FEBS Lett.; 1997; 414: 521–526. doi: 10.1016/S0014-5793(97)01062-4 PMID: 9323027

23. Johnsson B, Löfås S, Lindquist G. Immobilization of proteins to a carboxymethyldextran-modified gold surface for biospecific interaction analysis in surface plasmon resonance sensors. Anal Biochem. 1991; 198: 268–277. doi: 10.1016/0003-2697(91)90424-R PMID: 1724720

24. Andersson K, Hämäläinen M, Malmqvist M. Identification and optimization of regeneration conditions for affinity-based biosensor assays. A multivariate cocktail approach. Anal Chem. 1999; 71: 2475–2481. doi: 10.1021/ac981271j PMID: 10405611

25. Rodrigues RS, Izidoro LFM, Teixeira SS, Silveira LB, Hamaguchi A, Homsi-Brandeburgo MI, et al. Isolation and functional characterization of a new myotoxic acidic phospholipase A2 from *Bothrops pauloensis* snake venom. Toxicon. 2007; 50: 153–165. doi: 10.1016/j.toxicon.2007.03.005 PMID: 17451767

26. Altschul SF, Gish W, Miller W, Myers EW, Lipman DJ. Basic Local Alignment Search Tool. J Mol Biol. 1990; 215: 403–410. doi: 10.1016/S0022-2836(05)80360-2 PMID: 2231712

27. Thompson JD, Higgins DG, Gibson TJ. CLUSTAL W: improving the sensitivity of progressive multiple sequence alignment through sequence weighting, position-specific gap penalties and weight matrix choice. Nucleic Acids Res. 1994; 22: 4673–4680. doi: 10.1093/nar/22.22.4673 PMID: 7984417

28. Sali A, Blundell TL. Comparative protein modelling by satisfaction of spatial restraints. J Mol Biol. 1993; 234: 779–815. doi: 10.1006/jmbi.1993.1626 PMID: 8254673

29. Laskowski RA, MacArthur MW, Moss DS, Thornton JM. PROCHECK: a program to check the stereochemical quality of protein structures. J Appl Crystallogr. 1993; 26: 283–291. doi: 10.1107/S0021889892009944

30. Guex N, Peitsch MC. SWISS-MODEL and the Swiss-PdbViewer: An environment for comparative protein modeling. Electrophoresis. 1997; 18: 2714–2723. doi: 10.1002/elps.1150181505 PMID: 9504803

31. Pettersen EF, Goddard TD, Huang CC, Couch GS, Greenblatt DM, Meng EC, et al. UCSF Chimera—A visualization system for exploratory research and analysis. J Comput Chem. 2004; 25: 1605–1612. doi: 10.1002/jcc.20084 PMID: 15264254

32. Chen R, Li L, Weng Z. ZDOCK : An Initial-Stage Protein-Docking Algorithm. Proteins. 2003; 87: 80–87.

33. Fernandes CA, Marchi-Salvador DP, Salvador GM, Silva MCO, Costa TR, Soares AM, et al. Comparison between apo and complexed structures of bothropstoxin-I reveals the role of Lys122 and Ca^{2+}-binding loop region for the catalytically inactive Lys49-PLA$_2$s. J Struct Biol. 2010; 171: 31–43. doi: 10.1016/j.jsb.2010.03.019 PMID: 20371382

34. Dos Santos JI, Cintra-Francischinelli M, Borges RJ, Fernandes CAH, Pizzo P, Cintra ACO, et al. Structural, functional, and bioinformatics studies reveal a new snake venom homologue phospholipase A$_2$ class. Proteins Struct Funct Bioinforma. 2011; 79: 61–78. doi: 10.1002/prot.22858

35. Brenke R, Hall DR, Chuang G, Comeau SR, Bohnuud T, Beglov D, et al. Structural bioinformatics application of asymmetric statistical potentials to antibody—protein docking. Bioinformatics. 2012; 28: 2608–2614. doi: 10.1093/bioinformatics/bts493 PMID: 23053206

36. Kozakov D, Brenke R, Comeau SR, Vajda S. PIPER: an FFT-based protein docking program with pairwise potentials. Proteins. 2006; 65: 392–406. doi: 10.1002/prot.21117 PMID: 16933295

37. Ramachandran GN, Ramakrishnan C, Sasisekharan V. Stereochemistry of polypeptide chain configurations. J Mol Biol. 1963; 7: 95–99. doi: 10.1016/S0022-2836(63)80023-6 PMID: 13990617

38. Alvarenga L, Zahid M, Tommaso A, Juste M, Aubrey N, Billiald P, et al. Engineering venom's toxin-neutralizing antibody fragments and its therapeutic potential. Toxins (Basel). 2014; 6: 2541–2567. doi: 10.3390/toxins6082541

39. World Health Organisation. WHO Guidelines for the production control and regulation of snake antivenom immunoglobulins. 2010; 1–134. Available: http://www.who.int/bloodproducts/snake_antivenoms/en/

40. Guimarães CLS, Carvalho BMA, Fernandes CAH, Fontes MRM, Giglio JR, Barraviera B, et al. Alkylation of histidine residues of *Bothrops jararacussu* venom proteins and isolated phospholipases A$_2$: a biotechnological tool to improve the production of antibodies. Biomed Res Int. 2014; 2014:981923. doi: 10.1155/2014/981923 PMID: 24901004

41. Chotwiwatthanakun C, Pratanaphon R, Akesowan S, Sriprapat S, Ratanabanangkoon K. Production of potent polyvalent antivenom against three elapid venoms using a low dose, low volume, multi-site immunization protocol. Toxicon. 2001; 39: 1487–1494. doi: 10.1016/S0041-0101(01)00108-8 PMID: 11478956

42. Bakherad H, Gargari SLM, Rasooli I, Rajabibazl M, Mohammadi M, Ebrahimizadeh W, et al. In vivo neutralization of botulinum neurotoxins serotype e with heavy-chain camelid antibodies (VHH). Mol Biotechnol. 2013; 55: 159–167. doi: 10.1007/s12033-013-9669-1 PMID: 23666874

43. Thanongsaksrikul J, Srimanote P, Maneewatch S, Choowongkomon K, Tapchaisri P, Makino SI, et al. A VHH that neutralizes the zinc metalloproteinase activity of botulinum neurotoxin type A. J Biol Chem. 2010; 285: 9657–9666. doi: 10.1074/jbc.M109.073163 PMID: 20093370

44. Dumoulin M, Conrath K, Van Meirhaeghe A, Meersman F, Heremans K, Frenken LGJ, et al. Single-domain antibody fragments with high conformational stability. Protein Sci. 2002; 11: 500–515. doi: 10.1110/ps.34602 PMID: 11847273

45. Govaert J, Pellis M, Deschacht N, Vincke C, Conrath K, Muyldermans S, et al. Dual beneficial effect of interloop disulfide bond for single domain antibody fragments. J Biol Chem. 2012; 287: 1970–1979. doi: 10.1074/jbc.M111.242818 PMID: 22128183

46. Hmila I, Abdallah BAB, Saerens D, Benlasfar Z, Conrath K, Ayeb ME, et al. VHH, bivalent domains and chimeric Heavy chain-only antibodies with high neutralizing efficacy for scorpion toxin AahI' Mol Immunol. 2008; 45: 3847–3856. doi: 10.1016/j.molimm.2008.04.011 PMID: 18614235

47. Pereira MF, Novello JC, Cintra ACO, Giglio JR, Landucci ET, Oliveira B, et al. The amino acid sequence of bothropstoxin-II, an Asp-49 myotoxin from *Bothrops jararacussu* (Jararacucu) venom with low phospholipase A$_2$ activity. J Protein Chem. 1998; 17: 381–386. doi: 10.1023/A:1022563401413 PMID: 9619591

48. Janssen M, Freyvogel TA, Meier J. Antigenic relationship between the venom of the night adder *Causus maculatus* and venoms of other viperids. Toxicon. 1990; 28: 975–983 doi: 10.1016/0041-0101(90)90026-4 PMID: 1706897

49. Tan C, Tan N, Tan K, Kwong K. Antivenom cross-neutralization of the venoms of *Hydrophis schistosus* and *Hydrophis curtus*, two common sea snakes in Malaysian waters. Toxins (Basel). 2015; 7: 572–581. doi: 10.3390/toxins7020572

50. Lomonte B, Gutiérrez J, Ramírez M, Díaz C. Neutralization of myotoxic phospholipases A_2 from the venom of the snake *Bothrops asper* by monoclonal antibodies. Toxicon. 1992; 30: 239–245. doi: 10.1016/0041-0101(92)90866-4 PMID: 1382325

51. Kornhauser R, Isbister GK, O'Leary MA, Mirtschin P, Dunstan N, Hodgson WC. Cross-neutralisation of the neurotoxic effects of egyptian cobra venom with commercial tiger snake antivenom. Basic Clin Pharmacol Toxicol. 2013; 112: 138–143. doi: 10.1111/j.1742-7843.2012.00925.x PMID: 22788931

52. Cintra-Francischinelli M, Caccin P, Chiavegato A, Pizzo P, Carmignoto G, Angulo Y, et al. *Bothrops* snake myotoxins induce a large efflux of ATP and potassium with spreading of cell damage and pain. Proc Natl Acad Sci USA. 2010; 107: 14140–14145. doi: 10.1073/pnas.1009128107 PMID: 20660736

53. Fernandes CAH, Borges RJ, Lomonte B, Fontes MRM. A structure-based proposal for a comprehensive myotoxic mechanism of phospholipase A_2-like proteins from viperid snake venoms. Biochim Biophys Acta—Proteins Proteomics. 2014; 1844: 2265–2276. doi: 10.1016/j.bbapap.2014.09.015

54. Gutiérrez JM, Ownby CL. Skeletal muscle degeneration induced by venom phospholipases A_2: insights into the mechanisms of local and systemic myotoxicity. Toxicon. 2003; 42: 915–931. doi: 10.1016/j.toxicon.2003.11.005 PMID: 15019491

55. Mora-Obando D, Fernández J, Montecucco C, Gutiérrez JM, Lomonte B. Synergism between basic Asp49 and Lys49 phospholipase A_2 myotoxins of viperid snake venom *in vitro* and *in vivo*. PLoS One. 2014; 9: e109846. doi: 10.1371/journal.pone.0109846 PMID: 25290688

56. Arni RK, Ward RJ. Phospholipase A_2—a structural review. Toxicon. 1996; 34: 827–841. doi: 10.1016/0041-0101(96)00036-0 PMID: 8875770